ECOLOGY LETTERS

Ecology Letters, (2020) **23**: 881–890 doi: 10.1111/ele.13496

METHODS

Tracking long-distance migration of marine fishes using compound-specific stable isotope analysis of amino acids

Jun Matsubayashi,[1,2]* Yutaka Osada,[1,3]* Kazuaki Tadokoro,[4] Yoshiyuki Abe,[5,6] Atsushi Yamaguchi,[5] Kotaro Shirai,[6] Kentaro Honda,[7] Chisato Yoshikawa,[2] Nanako O. Ogawa,[2] Naohiko Ohkouchi,[2] Naoto F. Ishikawa,[2] Toshi Nagata,[6] Hiroomi Miyamoto,[4] Shigeto Nishino[2] and Ichiro Tayasu[1]

The peer review history for this article is available at https://publons.com/publon/10.1111/ele.13496

Abstract

The long-distance migrations by marine fishes are difficult to track by field observation. Here, we propose a new method to track such migrations using stable nitrogen isotopic composition at the base of the food web ($\delta^{15}N_{Base}$), which can be estimated by using compound-specific isotope analysis. $\delta^{15}N_{Base}$ exclusively reflects the $\delta^{15}N$ of nitrate in the ocean at a regional scale and is not affected by the trophic position of sampled organisms. In other words, $\delta^{15}N_{Base}$ allows for direct comparison of isotope ratios between proxy organisms of the isoscape and the target migratory animal. We initially constructed a $\delta^{15}N_{Base}$ isoscape in the northern North Pacific by bulk and compound-specific isotope analyses of copepods (n = 360 and 24, respectively), and then we determined retrospective $\delta^{15}N_{Base}$ values of spawning chum salmon (*Oncorhynchus keta*) from their vertebral centra (10 sections from each of two salmon). We then estimated the migration routes of chum salmon during their skeletal growth by using a state-space model. Our isotope tracking method successfully reproduced a known chum salmon migration route between the Okhotsk and Bering seas, and our findings suggest the presence of a new migration route to the Bering Sea Shelf during a later growth stage.

Keywords

Bering Sea Shelf, copepods, isoscape, migration, North Pacific, salmon, $\delta^{15}N_{Base}$.

Ecology Letters (2020) **23**: 881–890

INTRODUCTION

Long-distance migrations by highly mobile animals are one of the most stunning and threatened biological phenomena in the world, and have long fascinated scientists (Huntsman 1948; Abrahms *et al*. 2019). These migrations also play important ecological roles by increasing nutrient flow and connectivity between disparate locations (Bauer & Hoye 2014); however, they are highly vulnerable to disruption by habitat alterations caused by ongoing climate change (Berger 2004; Robinson *et al*. 2009). Tracking the migration routes of highly migratory animals is a necessary step to predict the impact of climate change as well as to boost understanding of the ultimate evolutionary drivers for such migratory behaviour.

Long-distance migrations are common across many taxa (Brower 1995; Robinson *et al*. 2009; Block *et al*. 2011). Unfortunately, many of these taxa, including marine animals, are difficult to track using field observation. Most of our knowledge of marine animal migration is based on fishing surveys, tagging studies and telemetry data (e.g. Carey & Scharold 1990; Quinn & Myers 2004; Semmens *et al*. 2007). However, there are several shortcomings to these techniques, including the enormous effort, cost, and difficulty of data collection, the limited life and detection range of biologging devices, and limitations on the body size of target animals (Cooke *et al*. 2013). Recently, stable isotope analysis has attracted attention as a new tool that could overcome these limitations in marine animals (e.g. Trueman *et al*. 2012; Trueman & St. John Glew 2019).

Isotope ratios in organism tissues often serve as intrinsic markers of habitat because environmental isotope ratios of one or more elements (usually) differ among geographic locations (e.g. Hobson 1999; Bowen *et al*. 2005; Bowen 2010). Data on spatial gradients in isotope ratios of a specific element can be used to draw what is known as an 'isoscape' (Bowen 2010). To be useful in the study of animal migration, the specific isotope used to construct an isoscape must meet the following criteria (Hobson et al. 2010): (1) substantial spatial variations are found in isotope ratios within the animal's habitat range, (2) isotope fractionation between the ambient environment and animal tissue can be corrected, and (3) the time period of spatial integration corresponding to a particular animal tissue is known. Stable nitrogen isotope ratios ($\delta^{15}N$) at the base of the food web ($\delta^{15}N_{Base}$) may meet these criteria in marine ecosystems.

[1]*Research Institute for Humanity and Nature, 457-4 Motoyama, Kamigamo, Kita-ku, Kyoto 603-8047, Japan*
[2]*Japan Agency for Marine-Earth Science and Technology, 2-15 Natsushima-Cho, Yokosuka, Kanagawa 237-0061, Japan*
[3]*Graduate School of Life Sciences, Tohoku University, 6-3 Aramaki-Aoba, Aoba-ku, Sendai, Miyagi 980-8578, Japan*
[4]*Tohoku National Fisheries Research Institute, Japan Fisheries Research and Education Agency, 3-27-5, Shinhama-cho, Shiogama, Miyagi 985-0001, Japan*
[5]*Graduate School of Fisheries Sciences, Hokkaido University, 3-1-1 Minatomachi, Hakodate, Hokkaido 041-8611, Japan*
[6]*Atmosphere and Ocean Research Institute, The University of Tokyo, 5-1-5, Kashiwanoha, Kashiwa-shi, Chiba 277-8564, Japan*
[7]*Hokkaido National Fisheries Research Institute, Japan Fisheries Research and Education Agency, 2-2 Nakanoshima, Toyohira-ku, Sapporo, Hokkaido, 062-0922, Japan*
**Correspondence: E-mail: matsu-jun@jamstec.go.jp and yosada@gmail.com*

$\delta^{15}N_{Base}$ values are calculated through $\delta^{15}N$ analysis of amino acids ($\delta^{15}N_{AAs}$; a technique that is often used to estimate trophic position [TP] in marine animals) by correcting for TP-dependent $\delta^{15}N$ increases in phenylalanine ($\delta^{15}N_{Phe}$). Unlike $\delta^{15}N$ values in bulk tissue ($\delta^{15}N_{Bulk}$), which increase with TP (DeNiro & Epstein 1981; Minagawa & Wada 1984), $\delta^{15}N_{Base}$ reflects the $\delta^{15}N$ of nitrate consumed by phytoplankton at a regional scale (Ohkouchi *et al.* 2017). Therefore, it is not influenced by the TP of the sampled organism. Substantial spatial variations in $\delta^{15}N_{Base}$ are likely to exist within the North Pacific because several studies have shown large spatial variations in nitrate $\delta^{15}N$ in the region (e.g. Schell *et al.* 1998; Pomerleau *et al.* 2014; Yoshikawa *et al.* 2018). Thus, $\delta^{15}N_{Base}$ meets criteria (1) and (2).

Recent studies have developed a method to perform retrospective $\delta^{15}N$ analysis in teleost fishes using their vertebrae (Matsubayashi *et al.* 2017, 2019). Fish vertebrae exhibit incremental growth, and isotopes incorporated into the bone collagen of each vertebral section remain in place for a long time in the absence of active metabolic tissue replacement. For this reason, segmental isotope analysis of vertebral sections can reconstruct retrospective $\delta^{15}N_{Base}$ values during periods of skeletal growth, satisfying criterion (3). Owing to these advantages, $\delta^{15}N_{Base}$ values can be a direct indicator of migration routes in fishes and other marine animals.

Here, we present a new method for identifying the migration route of highly migratory marine fishes by using $\delta^{15}N_{Base}$ isoscapes in conjunction with retrospective isotope analysis of individuals. We chose chum salmon (*Oncorhynchus keta*) as the target fish in this study. The species' migrations are known to take individuals over 10,000 km offshore of their natal streams (Swain *et al.* 1962; Urawa *et al.* 2000, 2005; Seeb *et al.* 2004). In previous studies, the migration routes of Asian populations of chum salmon were investigated by conducting extensive fishing surveys in the North Pacific (Urawa *et al.* 2000, 2005; Seeb *et al.* 2004). These studies caught salmon at multiple sampling stations in the North Pacific in several seasons, and investigated their origin by genetic analysis. They suggested that chum salmon initially run to the Okhotsk Sea after their seaward migration until late autumn, then migrate to the Western Subarctic Gyre in winter, and move to the Bering Sea by the following summer. Then, they come and go between the Bering Sea and Alaska Gyre in summer and winter, respectively, for several years. Finally, mature chum salmon return to Japan from the Bering Sea at around ocean age 4 (Fig. S1).

We constructed an isoscape of $\delta^{15}N_{Base}$ in the North Pacific using the $\delta^{15}N_{Bulk}$ and $\delta^{15}N_{AAs}$ of copepods collected from the migration area of chum salmon. Then, we performed retrospective $\delta^{15}N_{AAs}$ analysis of vertebral sections extracted from bodies of spawning salmon, and measured $\delta^{15}N_{Base}$ for successive growth stages of each fish (Matsubayashi *et al.* 2017, 2019). Finally, we developed a state-space model to estimate migration routes of individual salmon by using $\delta^{15}N_{Base}$ isoscapes in the North Pacific and $\delta^{15}N_{Base}$ time-series in salmon, and compared the results with a known migration route of chum salmon from Japan to the Bering Sea.

MATERIALS AND METHODS

Zooplankton and chum salmon sample collection

Zooplankton samples were obtained from the Odate Collection (Odate 1994) ($n = 305$; sampled from 2000 to 2018) of Fisheries Research and Education Agency (FRA), and additional samples were collected by the Hokkaido University training ship (*Oshoro Maru*; $n = 32$) in 2002 and 2012. They were stored in formalin until analysis; according to Ogawa *et al.* (2013), formalin preservation does not influence the $\delta^{15}N$ values of bulk and compound-specific isotope analyses. We also obtained frozen zooplankton samples ($n = 17$) from the Hokkaido National Fisheries Research Institute. These samples were collected during a 2017 cruise of the *Hokko Maru* in the Bering Sea. From each sample bottle, we selected one of the following six copepod species, which are dominant in the North Pacific: *Neocalanus cristatus*, *N. plumchrus*, *N. flemingeri*, *Oncaea venusta*, *Paracalanus parvus*, and *P. aculeatus* (Table S1). Copepod samples were rinsed with pure water twice and freeze-dried. Then, we removed the gut of large copepods (*N. cristatus*, *N. plumchrus*, and *N. flemingeri*) and placed the copepods in tin capsules for isotope analysis. Because it is technically difficult to excise the gut contents of small copepods (*Oncaea venusta*, *Paracalanus parvus*, and *P. aculeatus*), we used whole body samples of these species for isotope analysis. These six species have relatively long lifespans ranging from 1 month to 2 years (Paffenhöfer 1993; Tsuda *et al.* 2001), which enables us to obtain time-averaged isotopic information. We also collected $\delta^{15}N_{bulk}$ data for these species from existing literature (Pomerleau *et al.* 2014).

Bone samples were obtained from three individuals of chum salmon (IDs: OK1–3) collected at the Nukkibetsu River, Hokkaido, Japan (42.59 °N, 140.70 °E), in December 2016. We could not identify the age, sex, or origin (wild or hatchery reared) of these samples because we were not provided with any non-bone tissues. We also obtained three individuals of chum salmon from the Chitose River, Hokkaido (42.80 °N, 141.56 °E, IDs: OK4–6) from the Hokkaido National Fisheries Research Institute, FRA, as well as two individuals from the Otsuchi River (39.37 °N, 141.90 °E, IDs: OK7–8), Iwate, Japan. All salmon from the Chitose River were identified as hatchery salmon based on their otolith labels, whereas the origin of salmon from the Otsuchi River was unclear. Age and sex were identified for samples of both origins (Table S2). We extracted vertebral centra from each salmon, subdivided them into 10 sections and extracted bone collagen from the sections (see Text S1).

Stable nitrogen isotope analysis of bulk tissue

The stable isotope ratios of nitrogen for all samples were measured using one of two elemental analyser/isotope-ratio mass spectrometry systems depending on the volume of each sample (see Text S2). Stable isotope ratios are expressed in δ notation in accordance with the international standard scale, on the basis of the following equation:

$$\delta^{15}N_{Bulk} = R_{sample}/R_{standard} - 1, \quad (1)$$

where R_{sample} is the $^{15}N/^{14}N$ ratio of the sample, and $R_{standard}$ is that of atmospheric nitrogen. The $\delta^{15}N$ values were

calibrated against those of alanine A ($\delta^{15}N$ = –2.89‰; CERKU-01), alanine B ($\delta^{15}N$ = 22.71‰; CERKU-02), and threonine ($\delta^{15}N$ = –2.88‰; CERKU-05) laboratory standards (Tayasu *et al*. 2011). The maximum analytical standard deviations (SD) of these standards were lower than 1.07‰ for alanine A (n = 40), 0.63‰ for alanine B (n = 54), and 0.15‰ for threonine (n = 8).

Stable nitrogen isotope analysis of amino acids

The $\delta^{15}N_{AAs}$ measurements were performed only for some copepods and chum salmon samples to minimize experimental effort. Specifically, the sample size of salmon used for $\delta^{15}N_{AAs}$ measurements was strictly limited because it requires a ten-fold increase in the number of bone collagen samples due to retrospective isotope analysis. For this reason, we selected a representative three to six samples from six copepod species for $\delta^{15}N_{AAs}$ measurements so as to cover the $\delta^{15}N_{Bulk}$ range of each species, and collagen samples from the bone sections of two individuals of *O. keta* (IDs: OK2 and OK8) were used for $\delta^{15}N_{AAs}$ measurements. Samples for $\delta^{15}N_{AAs}$ were prepared based on amino acid derivatisation procedures, and the $\delta^{15}N_{AAs}$ values were determined by gas chromatography/combustion/isotope-ratio mass spectrometry (See Text S3).

Calculation of trophic position and $\delta^{15}N_{Bulk}$ of each sample

Trophic position (TP) of samples with $\delta^{15}N_{AAs}$ data were estimated based on differences in $\delta^{15}N$ between glutamic acid and phenylalanine as follows (Chikaraishi *et al*. 2009):

$$TP_{Glu-Phe} = \left(\delta^{15}N_{Glu} - \delta^{15}N_{Phe} - 3.4\right)/7.6 + 1, \quad (2)$$

where $\delta^{15}N_{Glu}$ and $\delta^{15}N_{Phe}$ represent the $\delta^{15}N$ values of glutamic acid and phenylalanine, respectively. We also calculated $\delta^{15}N_{Base}$ by using the estimated $TP_{Glu\text{-}Phe}$ and the trophic discrimination factor of phenylalanine (0.4‰) as follows:

$$\delta^{15}N_{Base} = \delta^{15}N_{Phe} - 0.4 \times (TP_{Glu-Phe} - 1). \quad (3)$$

We then performed linear regression analysis to explain variations in the $\delta^{15}N_{Base}$ of each species as a function of $\delta^{15}N_{Bulk}$ as follows:

$$\delta^{15}N_{Base} = \delta^{15}N_{Bulk} \times a + b, \quad (4)$$

where a and b were derived from the liner regression equation. In cases where the correlation between $\delta^{15}N_{Base}$ and $\delta^{15}N_{Bulk}$ in each equation was high (i.e., $r^2 > 0.8$; see Fig. S2), the regression equations were used to calculate $\delta^{15}N_{Base}$ values of copepod samples for which $\delta^{15}N_{AAs}$ was not measured.

Construction of a $\delta^{15}N_{Base}$ isoscape

$\delta^{15}N_{Base}$ values estimated from copepod $\delta^{15}N_{Bulk}$ and $\delta^{15}N_{AAs}$ were interpolated by using Data Interpolating Variational Analysis (DIVA) gridding software (Barth *et al*. 2010), and were visualized with Ocean Data View version 5.0.0 (ODV: Brown 1998; Schlitzer 2002). DIVA takes into account coastlines and bathymetric features and subdivides the domain on which estimation is performed. DIVA parameters for the interpolation were as follows: mapping range = 30–75°N and 135 °E–140 °W; scale lengths (x, y) = 30, 30; quality limit (standard deviation) = 1.5; signal-to-noise ratio = 40; depth of isosurface = 20 m; outliers excluded. Coastlines in the maps were based on the Global Self-consistent Hierarchical High-resolution Shorelines database v 2.1 (Wessel & Smith 1996). Deviations between measured (from copepod samples) and predicted (using DIVA gridding software) $\delta^{15}N_{Base}$ were also calculated by using ODV.

As a potential explanatory variable for spatial gradients in zooplankton $\delta^{15}N_{Base}$, we also estimated phytoplankton $\delta^{15}N$ ($\delta^{15}N_{esPhy}$) in the summer across the North Pacific using nitrate utilisation data (see Text S4, Fig. S3). We estimated $\delta^{15}N_{esPhy}$ for each data point by using Supplementary Equation (1), and interpolated the data onto a 1° grid throughout the North Pacific (Fig. S3). We did not estimate $\delta^{15}N_{esPhy}$ in areas of the eastern Bering Sea where the water depth is less than 100 m, as sedimentary denitrification also influences $\delta^{15}N_{esPhy}$ in such regions. Then, we calculated average $\delta^{15}N_{Base}$ in each 1° grid so that $\delta^{15}N_{Base}$ and $\delta^{15}N_{esPhy}$ could be compared at the same spatial scale. A scatter plot of these gridded isotopic values suggested that $\delta^{15}N_{Base}$ and $\delta^{15}N_{esPhy}$ are nonlinearly related (Fig. S4). For this reason, we fitted a linear regression using a squared term of $\delta^{15}N_{esPhy}$, and the best model was selected based on the Akaike Information Criterion (AIC). The modeling procedure was conducted using R version 3.5.3 (R Core Team 2019).

Estimation of chum salmon migration routes

We developed a state-space model to estimate the location (i.e., latitude and longitude) of each individual salmon at each growth stage (i.e., vertebral section) using the $\delta^{15}N_{Base}$ isoscape and retrospective $\delta^{15}N_{Base}$ values of salmon. Our model relies on several key assumptions. First, vertebral stable isotope ratios of chum salmon can be compared with those of the isoscape. This assumption is needed in order to conclude that a chum salmon existed at a location whose isotope value on the isoscape is similar to that of the vertebral section, and it is supported by our contention that the $\delta^{15}N_{Base}$ cancels the trophic discrimination between diet and consumer, and exclusively reflects the isotopic values in specific geographic locations. It is important to note that this assumption also provides the implicit model constraint that chum salmon cannot migrate outside of the constructed isoscape. Second, isotope values in each vertebral section are unchanged from the values at the time when each section was created. Matsubayashi *et al*. (2017, 2019) provided evidence of a minimal effect from replacement-based turnover in collagen from vertebral bone in fishes. Third, the natal river of individual salmon is the same as the sampled river. This assumption was based on the highly developed homing ability of chum salmon. Lastly, we assumed that the spatial scale at which chum salmon migrate is related to the growth stage of each individual, as has been shown in sockeye salmon (*O. nerka*) (Brett 1965). Using these assumptions, our model describes the spatial scale of migration as a linear function of the number of vertebral sections as counted from the vertebral centra (as explained below). In this model, we did not account for

individual variations in migration spatial scale because the number of individuals used for $\delta^{15}N_{AAs}$ was small ($n = 2$).

A time lag exists between the consumer feeding on a specific prey and the atoms from that prey being incorporated into the fish's bone collagen, although the length of this time lad has not been assessed. Therefore, our model estimates the location of salmon at which the unknown assimilation time lag has been subtracted from the time when each vertebral section was created. Let $x_{i,j}$ be the location (i.e., latitude and longitude) at which individual i consumed the prey before the lapse of the unknown assimilation time lag from vertebral section j was created (index j is the number of the vertebral section as counted from the centre of vertebral centra). Because chum salmon migrated from $x_{i,j-1}$ to $x_{i,j}$ at their growth stage $j-1$, it is biologically plausible to assume that $x_{i,j}$ is likely to be in the vicinity of $x_{i,j-1}$. This assumption is often used in ecological models that infer the movements of organisms. Thus, the probability with which each individual at each growth stage existed at location $x_{i,j}$ on an isoscape can be written as follows using the formula for a Gaussian distribution:

$$p\left(x_{i,j}|x_{i,j-1},\alpha_j^2\right)=\frac{1}{\sqrt{2\pi\alpha_{j-1}^2}}\exp\left(\frac{d\left(x_{i,j-1},x_{i,j}\right)^2}{2\alpha_{j-1}^2}\right), \quad (5)$$

where α_j is the migration scale when section j was created, and $d(x_1, x_2)$ represents the geographic distance between x_1 and x_2. Using the last assumption explained above, the migration spatial scale is formulated as a linear function of the number of vertebral sections from the vertebral centra:

$$\alpha_j=\exp(a+b\log(j+1)), \quad (6)$$

where a and b are the intercept and coefficient of the linear function, respectively. We defined the migration spatial scale at the initial growth stage as $\exp(a)$. Positive b values indicate that the migration spatial scale increases with somatic growth, and vice versa. Brett (1965) used a similar exponential formulation to describe the relationship between cruising speed and body size in salmon. To model the probability at which the $\delta^{15}N_{Base}$ of the vertebral sections, $y_{i,j}$, is observed at a location, $x_{i,j}$, on the isoscape, we used the formula for a Gaussian distribution as follows:

$$p\left(y_{i,j}|x_{i,j},\sigma_{i,j}^2\right)=\frac{1}{\sqrt{2\pi\sigma_{i,j}^2}}\exp\left(\frac{\left(y_{i,j}-g\left(x_{i,j}\right)\right)^2}{2\sigma_{i,j}^2}\right), \quad (7)$$

where $\sigma_{i,j}^2$ is the mean squared errors of the $\delta^{15}N_{Base}$ (bone collagen and isoscape), and $g(x)$ represents the $\delta^{15}N_{Base}$ of location x on the isoscape.

Our model was assimilated using a numerical integration filter algorithm (Kitagawa 1987), which allows us to analytically compute the likelihood of a non-linear state-space model. To implement the numerical integration filter, the constructed isoscape was discretized into 5777 grid cells of dimensions 0.5 degrees latitude by 0.5 degrees longitude. The geographic distance between grid-cell centres was computed using the R packages 'geosphere' (version 1.5-10, Hijmans 2019) and 'igraph' (version 1.2.4.2, Csardi & Nepusz 2006). All statistical analyses were conducted using R version 3.5.3 (R Core Team 2019). Migration routes were estimated for two individual salmon (IDs: OK2 and OK8) that were sampled for $\delta^{15}N_{AAs}$ analysis.

RESULTS

Construction of a $\delta^{15}N_{Base}$ isoscape

We obtained $\delta^{15}N_{Bulk}$ and $\delta^{15}N_{AAs}$ values for six copepod species (*N. cristatus*: $n = 123$ and 6, respectively; *N. plumchrus*: $n = 54$ and 5; *N. flemingeri*: $n = 27$ and 3; *O. venusta*: $n = 43$ and 3; *P. aculeatus*: $n = 11$ and 5; *P. parvus*: $n = 77$ and 3), from our own samples ($n = 354$) and data from the literature (Pomerleau *et al.* 2014) ($n = 6$). Based on $\delta^{15}N_{AAs}$, the mean TPs of each copepod species were 2.7 (range: 2.5–2.9) for *N. cristatus*, 2.6 (2.4–2.9) for *N. plumchrus*, 2.7 (2.4–2.8) for *N. flemingeri*, 2.2 (2.1–2.5) for *O. venusta*, 2.3 (1.9–2.6) for *P. parvus*, and 1.9 (1.9–2.0) for *P. aculeatus* (Table S3). The $\delta^{15}N_{Base}$ and $\delta^{15}N_{Bulk}$ were highly correlated in each species ($r^2 = 0.905$ for *N. cristatus*, 0.827 for *N. plumchrus*, 0.993 for *N. flemingeri*, 0.974 for *O. venusta*, 0.871 for *P. parvus*, and 0.818 for *P. aculeatus*; Fig. S2). Therefore, the $\delta^{15}N_{Base}$ values were calculated using the regression equations with $\delta^{15}N_{Bulk}$ data (eqn 4). The slope and intercept of the species (a and b in eqn 4) were 1.455 and –6.128 for *N. cristatus*, 1.229 and –7.010 for *N. plumchrus*, 1.866 and –11.496 for *N. flemingeri*, 2.400 and –11.028 for *O. venusta*, 0.977 and –5.242 for *P. parvus*, and 1.461 and –6.590 for *P. aculeatus*, respectively (Fig. S2).

The estimated isoscape showed a large spatial variation in $\delta^{15}N_{Base}$ in our study area (see Fig. 1). Specifically, the $\delta^{15}N_{Base}$ was different among the Okhotsk Sea and coastal area of Japan (2.5–5.0‰), the central North Pacific (–5.0‰ to 0.0‰) and the Bering Sea Shelf (5.0–8.0‰). Linear regression analysis showed that spatial gradients in $\delta^{15}N_{Base}$ were largely explained by $\delta^{15}N_{esPhy}$ (explained deviance: 45.3%, Fig. S4). Therefore, estimated $\delta^{15}N_{esPhy}$ complemented $\delta^{15}N_{Base}$ values in areas of chum salmon habitat where zooplankton samples were not available, such as the Okhotsk Sea and Gulf of Alaska (Fig. 1). The root-square-mean error in $\delta^{15}N_{Base}$ values between actual measurements (copepod samples) and values predicted by DIVA gridding software was 1.42‰.

Retrospective stable isotope analysis of chum salmon

All sampled individuals shared common trends in $\delta^{15}N_{Bulk}$ along the vertebral axis (Fig. 2): $\delta^{15}N_{Bulk}$ values were almost identical (mean ± SD: 10.5‰ ± 0.3‰) in Section 1 (closest to the middle of the centrum) among sampled individuals, then gradually decreased from the centre to middle sections, increased rapidly in the marginal sections, and finally reached the highest value in the last section (12.7‰ ± 0.7‰; Table S4).

The $\delta^{15}N_{AAs}$ showed that the TP in the bone sections of OK2 and OK8 ranged from 3.0 to 3.5 and from 3.0 to 3.4, respectively, and no clear trends along the growing axis of vertebral sections were found (Table S4). The $\delta^{15}N_{Base}$ and $\delta^{15}N_{Bulk}$ values of vertebral sections of the two salmon

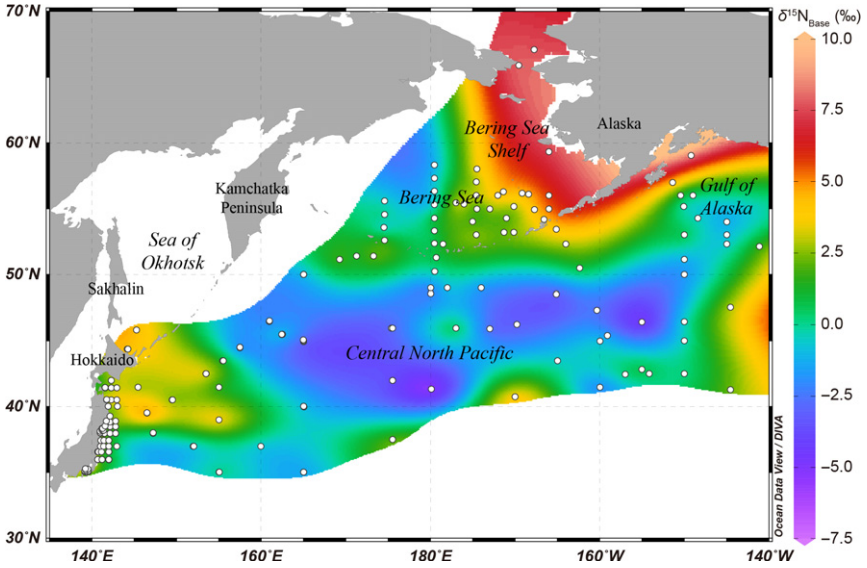

Figure 1 Map of the estimated $\delta^{15}N_{Base}$ isoscape showing the location of zooplankton sampling sites (white circles).

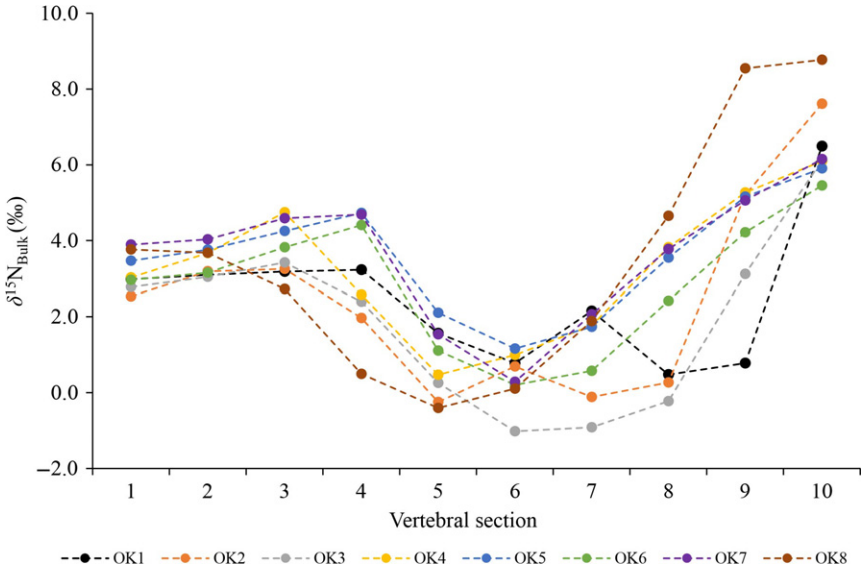

Figure 2 Patterns in $\delta^{15}N_{Bulk}$ along the vertebral sections of sampled Japanese chum salmon (IDs: OK1–8). Vertebral bone sections (*x*-axis) are numbered from the centre of the vertebral centrum and increase toward the margin.

individuals were highly correlated ($r^2 = 0.754$ for OK2 and 0.916 for OK8).

Estimation of chum salmon migration routes

The estimated spatial scale of migration in salmon suggests that their mobility increases with somatic growth ($a = 5.189 \pm 0.118$ and $b = 0.881 \pm 0.143$, Fig. S5). The state-space model successfully reproduced the long-distance migration of two chum salmon individuals from the western North Pacific (Fig. 3, orange areas in panels 1–5) to the Bering Sea (Fig. 3, orange areas in panels 6–9), supporting a previously reported migration pattern for this species (Urawa *et al*. 2000, 2005; Seeb *et al*. 2004). In addition, we found that both salmon individuals migrated onto the Bering Sea Shelf during the later stages of their growth (Fig. S5).

DISCUSSION

$\delta^{15}N_{Base}$ isoscapes in the North Pacific

Our isoscape shows that the eastern Bering Sea continental shelf has higher $\delta^{15}N_{Base}$ ($\delta^{15}N_{Base} > 7.0‰$; Fig. 1) than any other potential habitat range of chum salmon. This high $\delta^{15}N_{Base}$ is likely to be a result of coupled partial nitrification–denitrification in this region (Brown *et al*. 2015). High rates of sedimentary denitrification fueled by active nitrification preferentially remove ^{14}N from the system, thereby

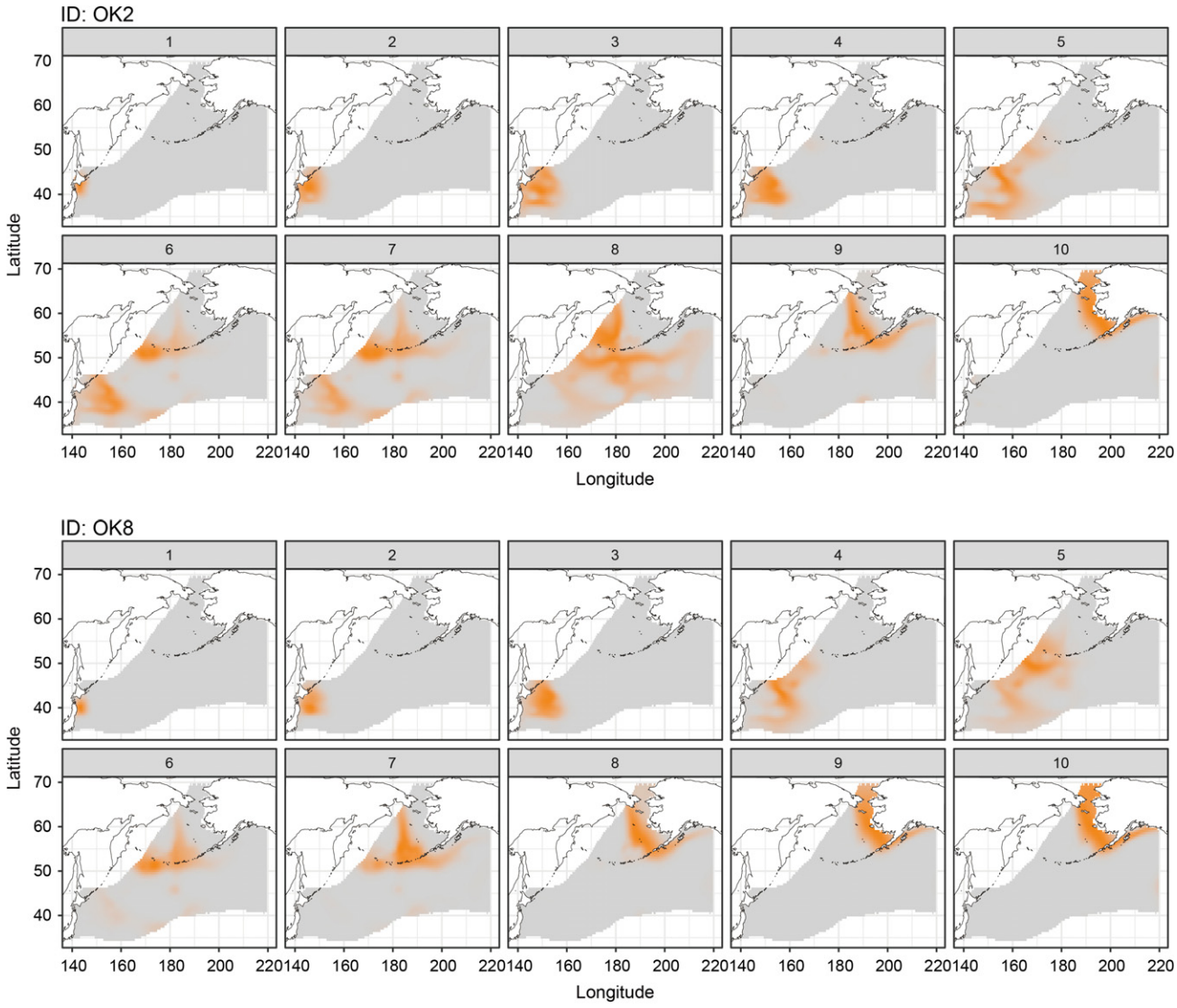

Figure 3 Estimated chum salmon migration areas. Mean presence probabilities for two salmon individuals (IDs: OK2 and OK8) at growth stages 1–10 (panels 1–10, respectively). The colour gradients (tints of orange) indicate presence probability (low to high). The grey area shows the extent of the isoscape.

enriching ^{15}N in the remaining nitrate (Granger *et al.* 2011). Spatial patterns of $\delta^{15}N_{Base}$ in the pelagic subarctic North Pacific are largely determined by nitrate utilisation, which is the ratio of nitrate assimilation by phytoplankton to nitrate supply in the euphotic layer, and is inversely correlated with surface water nitrate concentrations because of isotope fractionation during nitrate assimilation by phytoplankton (Fig. S3). In the western subarctic North Pacific, which is a nutrient-rich, low-chlorophyll region, nitrate is not depleted throughout the year and phytoplankton growth is instead limited by the availability of other micronutrients, such as iron (Nishioka & Obata 2017). This results in less fractionation associated with nitrate utilisation, which in turn accounts for the low $\delta^{15}N_{Base}$ in the Western Subarctic North Pacific (Yoshikawa *et al.* 2018). Nitrate concentrations decrease with distance from the nutrient-rich, low-chlorophyll region and nitrate $\delta^{15}N$ increases with nitrate depletion (Yoshikawa *et al.* 2018), which may account for the increased $\delta^{15}N_{Base}$ around the eastern coast of Japan and the Gulf of Alaska. Unfortunately, the isoscape compiled in this study suffers from a paucity of data in the Okhotsk Sea and the western Bering Sea Shelf. Although previous studies have suggested that nitrate $\delta^{15}N$ in the Okhotsk Sea is similar to that of the eastern coast of Japan and not as high as that of the Bering Sea Shelf (Yoshikawa *et al.* 2006), it remains possible that $\delta^{15}N_{Base}$ in the western Bering Sea Shelf resembles that of the eastern Bering Sea Shelf. Thus, we cannot discount the possibility that the salmon analysed in this study migrated to the western Bering Sea Shelf, although this would not affect the substance of our conclusions.

Our results also suggest that $\delta^{15}N_{Base}$ can be used as a direct indicator of the origin of marine organisms as suggested by previous studies (Hetherington *et al.* 2017; McMahon & Newsome 2019). This is supported by $\delta^{15}N_{Base}$ values in the

first vertebral section (Section 1) of two salmon (OK2: 4.4‰ and OK8: 3.6‰) similar to that of the isoscape in coastal Japan and the Okhotsk Sea (ca. 4‰; Fig. 1). A previous study also confirmed that Japanese chum salmon initially move into the Okhotsk Sea just after their seaward migration (Urawa *et al*. 2009). Large seasonal variations in the isotopic composition of primary producers (Bronk *et al*. 1994; Rolff 2000; Hannides *et al*. 2009) often complicate estimations of the isotopic baseline in the ocean. However, copepods effectively provide time-averaged $\delta^{15}N_{Base}$ values in a given region because they have relatively long lifespans (from 1 month to 2 years) (Paffenhöfer 1993; Tsuda *et al*. 2001), low dispersal ability, and low intra-species TP variation (Table S3). In our study, copepod samples from the pelagic North Pacific were mostly composed of large *Neocalanus* species, which have a lifespan of 1–2 years (Tsuda *et al*. 2001). In coastal areas, we sampled copepods that have a shorter lifespan across different seasons to take any seasonal variation into account, and to capture the annual mean $\delta^{15}N_{Base}$ of each region.

Chum salmon migration routes

Our estimates of chum salmon migration routes successfully reproduced a known migration pattern from coastal Japan to the Bering Sea (Urawa *et al*. 2000, 2001; Seeb *et al*. 2004; Whittle *et al*. 2018). More importantly, it is likely that chum salmon move onto the Bering Sea Shelf at the last stage of their somatic growth. Although the number of chum salmon used for the $\delta^{15}N_{AAs}$ analysis is limited ($n = 2$), we observed similar isotopic profiles of $\delta^{15}N_{Bulk}$ in the vertebral sections of all the salmon we sampled ($n = 8$). Furthermore, some of these salmon born in different years (Table S2) shared the migration onto the Bering Sea Shelf, indicating that this migration pattern is not influenced by annual variation in the diets of chum salmon. Thus, our results suggest that the Bering Sea Shelf plays an important role for the growth at later stages of chum salmon in Japan. Note, however, that the migration routes estimated by stable isotope analysis did not reflect homing migrations to the Japanese coast from the Bering Sea, possibly because the vertebrae of the sampled individuals did not exhibit substantial growth during this homing migration.

Given that fish somatic growth generally stops after sexual maturation because they devote surplus energy to reproduction (Lester *et al*. 2004), salmon vertebrae are not likely to grow substantially after maturation; in other words, the timing of maturation corresponds to that of the formation of the last vertebral section (Section 10). Ishida *et al*. (1998) investigated the relationship between age and fork length in chum salmon and showed that they exhibit substantial somatic growth during sexual maturation (Fig. S6). Other physiological studies have also shown higher levels of growth hormone in maturing salmon than those in immature salmon (Björnsson 1994; Stead *et al*. 1999), although growth rates rapidly decrease in the late phase of maturation (Stead *et al*. 1999). Thus, our data indicate that salmon migration to the Bering Sea Shelf is strongly related to sexual maturation. The Bering Sea Shelf supports high phytoplankton productivity (Lester *et al*. 2004), which feeds one of the highest benthic faunal biomass densities in the world's oceans (Highsmith 1990; Grebmeier et al. 1995). Specifically, large euphausiid populations in the region should be an important food resource for maturing chum salmon (Moss *et al*. 2009). For this reason, this region is a suitable habitat to fulfill the nutritional demands of sexual maturation in salmon, and its productivity and environmental conditions may be key determinants of the age and size at maturation of the Japanese chum salmon, which have a large influence on individual fitness (Roff 1984; Mangel 1996).

Potential usefulness of isotope tracking for the study of marine animal migration

Our results demonstrate that an isotope tracking method using copepod-based $\delta^{15}N_{Base}$ isoscapes coupled with retrospective isotope analysis of vertebral sections has the potential to provide new insights into the migration routes of highly migratory marine fishes. So far, several studies have published marine isoscapes of light elements such as $\delta^{13}C$, $\delta^{15}N$, and $\delta^{34}S$ (McMahon *et al*. 2013; St. John Glew et al., 2019). However, bulk tissue analysis of these elements is generally unsuitable for migration tracking. This is because trophic discrimination factors between diet and consumer sometimes differ among species or tissues (Caut *et al*. 2010), making it difficult to calibrate isotopic values across these categories. This uncertainty in trophic discrimination factors is an important source of error in migration route or habitat estimates calculated from bulk tissue analysis of several species. $\delta^{15}N_{Base}$, on the other hand, sidesteps this issue because it exclusively reflects site-specific $\delta^{15}N$ values independently of the diet and species of target organisms.

In addition to the use of isoscapes of $\delta^{15}N_{Base}$, retrospective isotope analysis also greatly improves the precision of migration route estimates generated by isotope tracking when target animals move into an isotopically distinct area. One advantage of using the sequential analysis of vertebral sections is that it can provide a larger number of samples needed for multi-isotope analysis than otolith analysis. One disadvantage of using vertebral sections, however, is that isotopic records are only available for periods of skeletal growth. This is why no vertebral isotopic records were available for chum salmon migrating back to Japan from the Bering Sea Shelf, since chum salmon do not exhibit substantial skeletal growth after sexual maturation. Similarly, our isotope tracking did not detect winter migrations into the Gulf of Alaska, which are described in previous studies (Urawa *et al*. 2005, 2009). Several studies have revealed significantly lower growth hormone levels in chum salmon in the Gulf of Alaska than those in the Bering Sea (e.g. Onuma *et al*. 2010), suggesting that chum salmon do not exhibit substantial somatic growth in the Gulf of Alaska. Consequently, our results suggest that isotope tracking using bone collagen is a sensitive method for detecting foraging migrations, but may overlook other types such as winter and homing migrations.

Because the North Pacific is a hotspot for highly migratory marine animals (Block *et al*. 2011), our reported isoscape in this area can be a powerful tool for investigating long-distance

ocean migrations of other animals. One advantage of the isotope tracking method is that it can reveal migration routes of individual animals over a prolonged timescale (the timescale of bone growth). Although the spatial resolution of the method depends on the spatial scale of isotopic gradients among habitats, the use of additional isoscapes based on radiocarbon content (Larsen *et al*. 2018) or neodymium stable isotope ratios (Saitoh *et al*. 2018) could help enable finer-scale determinations of fish migration routes.

ACKNOWLEDGEMENTS

We thank I. Itoh and C. Kamata at the Tohoku National Fisheries Research Institute for the preparation of copepod samples; C. Yoshimizu at the Research Institute for Humanity and Nature for stable isotope analysis of bulk tissues; A. Matsuda and T. Kawakami at the University of Tokyo and K. Nakata and S. Yoshimasu at the Japan Fisheries Research and Education Agency for providing salmon samples for analysis; Y. Takano, T. Blattmann and anonymous reviewers for their helpful comments on the draft of this paper; the Foundation for the Japan Science and Technology Agency Core Research for Evolutional Science and Technology (JST CREST) Grant JPMJCR13A4 and JPMJCR13A3; the Japan Society for the Promotion of Science (JSPS) KAKENHI Grant 17J04991 and 19K20495 to J.M.; the Japanese Ministry of Education, Culture, Sports, Science and Technology (MEXT) the Arctic Challenge for Sustainability (ArCS) Project, and MEXT; Tohoku Ecosystem-Associated Marine Sciences Project Grant JPMXD1111105259 and JPMXD1111105260.

CONFLICT OF INTEREST

The authors declare no conflict of interest.

AUTHORSHIP

J.M., I.T. and Y.O. conceived this study; K.T., A.Y., K.S., K.H., H.M. and S.N. provided copepod samples and contextual information; J.M. and T.N. provided chum salmon samples and contextual information; J.M. performed sectioning of salmon vertebrae and collagen extraction from bone samples; J.M., N.O.O., N.F.I., N.O. and I.T. performed bulk and compound-specific stable nitrogen isotope analyses; C.Y. provided data for nitrate utilisation and phytoplankton stable nitrogen isotope ratios in the North Pacific; Y.O. developed a statistical model to estimate salmon migration routes; J.M., Y.O. and C.Y. wrote the first draft of the paper; all authors were involved in interpreting the results and contributed to the final draft of the paper; J.M. and Y.O. contributed equally to this work.

DATA AVAILABILITY STATEMENT

All stable isotope data for zooplankton and fish bone collagen are provided in the Supplementary Information. Raw isotopic data of zooplankton samples and fish bone collagen will be available from the Dryad Digital Repository: https://doi.org/10.5061/dryad.r6p27. The custom code used to estimate chum salmon migration routes is provided in the Supplementary Information.

REFERENCES

Abrahms, B., Hazen, E.L., Aikens, E.O., Savoca, M.S., Goldbogen, J.A., Bograd, S. *et al*. (2019). Memory and resource tracking drive blue whale migrations. *Proc. Natl Acad. Sci. USA*, 116, 5582–5587.

Barth, A., Alvera-Azcárate, A., Troupin, C., Ouberdous, M. & Beckers, J.M. (2010). A web interface for gridding arbitrarily distributed in situ data based on Data-Interpolating Variational Analysis (DIVA). *Adv. Geos*., 28, 29–37.

Bauer, S. & Hoye, B.J. (2014). Migratory animals couple biodiversity and ecosystem functioning worldwide. *Science*, 344, 1242552.

Berger, J. (2004). The last mile: how to sustain long-distance migration in mammals. *Conserv. Biol*., 18, 320–331.

Björnsson, B.T., Taranger, G.L., Hansen, T., Stefansson, S.O. & Haux, C. (1994). The interrelation between photoperiod, growth hormone, and sexual maturation of adult Atlantic salmon (*Salmo salar*). *Gen. Comp. Endocr*., 93, 70–81.

Block, B.A., Jonsen, I.D., Jorgensen, S.J., Winship, A.J., Shaffer, S.A., Bograd, S.J. *et al*. (2011). Tracking apex marine predator movements in a dynamic ocean. *Nature*, 475, 86–90.

Bowen, G.J. (2010). Isoscapes: Spatial pattern in isotopic biogeochemistry. *Annu. Rev. Earth. Planet. Sci*., 38, 161–187.

Bowen, G.J., Wassenaar, L.I. & Hobson, K.A. (2005). Global application of stable hydrogen and oxygen isotopes to wildlife forensics. *Oecologia*, 143, 337–348.

Brett, J.R. (1965). The relation of size to rate of oxygen consumption and sustained swimming speed of sockeye salmon (*Oncorhynchus nerka*). *J. Fish. Res. Board. Can*., 22, 1491–1501.

Bronk, D.A., Gilbert, P.M. & Ward, B.B. (1994). Nitrogen uptake, dissolved nitrogen release, and new production. *Science*, 265, 1843–1856.

Brower, L.P. (1995). Understanding and misunderstanding the migration of the monarch butterfly (*Nymphalidae*) in North America: 1857–1995. *J. Lepid. Soc*., 49, 304–385.

Brown, M. (1998). Ocean data view 4.0. *Oceanography*, 11, 19–21.

Brown, Z.W., Casciotti, K.L., Pickart, R.S., Swift, J.H. & Arrigo, K.R. (2015). Aspects of the marine nitrogen cycle of the Chukchi Sea shelf and Canada Basin. *Deep Sea Res. Part II Top. Stud. Oceanogr*., 118, 73–87.

Carey, F.G. & Scharold, J.V. (1990). Movements of blue sharks (*Prionace glauca*) in depth and course. *Mar. Biol*., 106, 329–342.

Caut, S., Angulo, E., Courchamp, F. & Figuerola, J. (2010). Trophic experiments to estimate isotope discrimination factors. *J. Appl. Ecol*., 47, 948–954.

Chikaraishi, Y., Ogawa, N.O., Kashiyama, Y., Takano, Y., Suga, H., Tomitani, A. *et al*. (2009). Determination of aquatic food-web structure based on compound-specific nitrogen isotopic composition of amino acids. *Limnol. Oceanogr. Meth*., 7, 740–750.

Cooke, S.J., Midwood, J.D., Thiem, J.D., Klimley, P., Lucas, M.C., Thorstad, E.B. *et al*. (2013). Tracking animals in freshwater with electronic tags: past, present and future. *Anim. Biotelem*., 1, 5.

R Core Team (2019). *R:* A language and environment for statistical computing. Retrieved from, R Foundation for Statistical Computing (Vienna, Austria). https://www.R-project.org/.

Csardi, G. & Nepusz, T. (2006). The igraph software package for complex network research. *Inter. Journal, Complex Systems*, p1695, http://igraph.org.

DeNiro, M.J. & Epstein, S. (1981). Influence of diet on the distribution of nitrogen isotopes in animals. *Geochim. Cosmochim. Ac*., 45, 341–351.

Granger, J., Prokopenko, M.G., Sigman, D.M., Mordy, C.W., Morse, Z.M., Morales, L.V. *et al*. (2011). Coupled nitrification-denitrification in sediment of the eastern Bering Sea shelf leads to ^{15}N enrichment of fixed N in shelf waters. *J. Geophys. Res. Oceans*., 116, C11006.

Grebmeier, J.M., Smith, W.O. Jr & Conover, R.J. (1995). Biological processes on Arctic continental shelves: ice-ocean biotic interactions. In: Smith, O. S. Jr, Grebmeier, J. M. (eds) *Arctic oceanography: marginal ice zones and continental shelves*. American Geophysical Union, Washington, DC, pp. 231–261.

Hannides, C.C.S., Popp, B.N., Landry, M.R. & Graham, B.S. (2009). Quantitative determination of zooplankton trophic position using amino acid-specific stable nitrogen isotope analysis. *Limnol. Oceanogr.*, 54, 50–61.

Hetherington, E.D., Olson, R.J., Drazen, J.C., Lennert-Cody, C.E., Ballance, L.T., Kaufmann, R.S. *et al.* (2017). Spatial food-web structure in the eastern tropical Pacific Ocean based on compound-specific nitrogen isotope analysis of amino acids. *Limnol. Oceanogr.*, 62, 541–560.

Highsmith, R.C. & Coyle, K.O. (1990). High productivity of northern Bering Sea benthic amphipods. *Nature*, 344, 862.

Hijmans, R.J. (2019). Geosphere: Spherical trigonometry. R package version 1.5-10. https://CRAN.R-project.org/package=geosphere.

Hobson, K.A. (1999). Tracing origins and migration of wildlife using stable isotopes: a review. *Oecologia*, 120, 314–326.

Hobson, K.A., Barnett-Johnson, R. & Cerling, T. (2010). *Using Isoscapes to Track Animal Migration. Isoscapes: Understanding Movement, Pattern and Processes on Earth Through Isotope Mapping*, Springer, New York, NY, pp. 273–298.

Huntsman, A.G. (1948). Salmon and animal migration. *Nature*, 161, 300–302.

Ishida, Y., Ito, S., Ueno, Y. & Sakai, J. (1998). Seasonal growth patterns of Pacific salmon (*Oncorhynchus* spp.) in offshore waters of the North Pacific Ocean. *N. Pac. Anadr. Fish. Comm. Bull.*, 1, 66–80.

Kitagawa, G. (1987). Non-gaussian state-space modeling of nonstationary time series. *J. Amer. Stat. Assoc.*, 82, 1032–1041.

Larsen, T., Yokoyama, Y. & Fernandes, R. (2018). Radiocarbon in ecology: Insights and perspectives from aquatic and terrestrial studies. *Meth. Ecol. Evol.*, 9, 181–190.

Lester, N.P., Shuter, B.J. & Abrams, P.A. (2004). Interpreting the von Bertalanffy model of somatic growth in fishes: the cost of reproduction. *Proc. R. Soc. Lond. Ser. B.*, 271, 1625–1631.

Mangel, M. (1996). Life history invariants, age at maturity and the ferox trout. *Evol. Ecol.*, 10, 249–263.

Matsubayashi, J., Saitoh, Y., Osada, Y., Uehara, Y., Habu, J., Sasaki, T. *et al.* (2017). Incremental analysis of vertebral centra can reconstruct the stable isotope chronology of teleost fishes. *Meth. Ecol. Evol.*, 8, 1755–1763.

Matsubayashi, J., Umezawa, Y., Matsuyama, M., Kawabe, R., Mei, W., Wan, X. *et al.* (2019). Using segmental isotope analysis of teleost fish vertebrae to estimate trophic discrimination factors of bone collagen. *Limnol. Oceanogr. Meth.*, 17, 87–96.

McMahon, K.W. & Newsome, S.D. (2019). *Amino Acid Isotope Analysis: A New Frontier in Studies of Animal Migration and Foraging Ecology. Tracking Animal Migration with Stable Isotopes*, London, UK, Academic Press, pp. 173–190.

McMahon, K.W., Hamady, L.L. & Thorrold, S.R. (2013). A review of ecogeochemistry approaches to estimating movements of marine animals. *Limnol. Oceanogr.*, 58, 697–714.

Minagawa, M. & Wada, E. (1984). Stepwise enrichment of ^{15}N along food chains: further evidence and the relation between δ^{15}N and animal age. *Geochim. Cosmochim. Ac.*, 48, 1135–1140.

Moss, J.H., Murphy, J.M., Farley, E.V., Eisner, L.B. & Andrews, A.G. (2009). Juvenile pink and chum salmon distribution, diet, and growth in the northern Bering and Chukchi seas. *N. Pac. Anadr. Fish. Comm. Bull.*, 5, 191–196.

Nishioka, J. & Obata, H. (2017). Dissolved iron distribution in the western and central subarctic Pacific: HNLC water formation and biogeochemical processes. *Limnol. Oceanogr.*, 62, 2004–2022.

Odate, T. (1994). Plankton abundance and size structure in the northern North Pacific Ocean in early summer. *Fish. Oceanogr.*, 3, 267–278.

Ogawa, N.O., Chikaraishi, Y. & Ohkouchi, N. (2013). Trophic position estimates of formalin-fixed samples with nitrogen isotopic compositions of amino acids: an application to gobiid fish (Isaza) in Lake Biwa. *Japan. Ecol. Res.*, 28, 697–702.

Ohkouchi, N., Chikaraishi, Y., Close, H.G., Fry, B., Larsen, T., Madigan, D.J. *et al.* (2017). Advances in the application of amino acid nitrogen isotopic analysis in ecological and biogeochemical studies. *Org. Geochem.*, 113, 150–174.

Onuma, T.A., Ban, M., Makino, K., Katsumata, H., Hu, W., Ando, H. *et al.* (2010). Changes in gene expression for GH/PRL/SL family hormones in the pituitaries of homing chum salmon during ocean migration through upstream migration. *Gen. Comp. Endocr.*, 166, 537–548.

Paffenhöfer, G.A. (1993). On the ecology of marine cyclopoid copepods (Crustacea, Copepoda). *J. Plank. Res.*, 15, 37–55.

Pomerleau, C., Nelson, R.J., Hunt, B.P., Sastri, A.R. & Williams, W.J. (2014). Spatial patterns in zooplankton communities and stable isotope ratios (δ^{13}C and δ^{15}N) in relation to oceanographic conditions in the sub-Arctic Pacific and western Arctic regions during the summer of 2008. *J. Plank. Res.*, 36, 757–775.

Quinn, T.P. & Myers, K.W. (2004). Anadromy and the marine migrations of Pacific salmon and trout: Rounsefell revisited. *Rev. Fish Biol. Fish.*, 14, 421–442.

Robinson, R.A., Crick, H.Q., Learmonth, J.A., Maclean, I.M., Thomas, C.D., Bairlein, F. *et al.* (2009). Travelling through a warming world: climate change and migratory species. *Endang. Species Res.*, 7, 87–99.

Roff, D.A. (1984). The evolution of life history parameters in teleosts. *Can. J. Fish. Aquat. Sci.*, 41, 989–1000.

Rolff, C. (2000). Seasonal variation in δ^{13}C and δ^{15}N of size-fractionated plankton at a coastal station in the northern Baltic proper. *Mar. Ecol. Prog. Ser.*, 203, 47–65.

Saitoh, Y., Nakano, T., Shin, K.C., Matsubayashi, J., Kato, Y., Amakawa, H. *et al.* (2018). Utility of Nd isotope ratio as a tracer of marine animals: regional variation in coastal seas and causal factors. *Ecosphere*, 9, e02365.

Schell, D.M., Barnett, B. A. & Vinette, K. A., (1998). Carbon and nitrogen isotope ratios in zooplankton of the Bering, Chukchi and Beaufort seas. *Mar. Ecol. Prog. Ser.*, 162, 11–23.

Schlitzer, R. (2002). Interactive analysis and visualization of geoscience data with Ocean Data View. *Comput. Geosci.*, 28, 1211–1218.

Seeb, L.W., Crane, P.A., Kondzela, C.M., Wilmot, R.L., Urawa, S., Varnavskaya, N.V. *et al.* (2004). Migration of Pacific Rim chum salmon on the high seas: insights from genetic data. *Environ. Biol. Fish.*, 69, 21–36.

Semmens, J.M., Pecl, G.T., Gillanders, B.M., Waluda, C.M., Shea, E.K., Jouffre, D. *et al.* (2007). Approaches to resolving cephalopod movement and migration patterns. *Rev. Fish Biol. Fish.*, 17, 401.

St. John Glew, K., Graham, L. J., McGill, R. A. and Trueman, C. N. (2019). Spatial models of carbon, nitrogen and sulphur stable isotope distributions (isoscapes) across a shelf sea: An INLA approach. *Meth. Ecol. Evol.*, 10, 518–531.

Stead, S.M., Houlihan, D.F., McLay, H.A. & Johnstone, R. (1999). Food consumption and growth in maturing Atlantic salmon (*Salmo salar*). *Can. J. Fish. Aquat. Sci.*, 56, 2019–2028.

Swain, A., Hartley, W.G. & Davies, R.B. (1962). Long-distance migration of salmon. *Nature*, 195, 1122.

Tayasu, I., Hirasawa, R., Ogawa, N.O., Ohkouchi, N. & Yamada, K. (2011). New organic reference materials for carbon and nitrogen-stable isotope ratio measurements provided by Center for Ecological Research, Kyoto University, and Institute of Biogeosciences, Japan Agency for Marine-Earth Science and Technology. *Limnology*, 12, 261–266.

Trueman, C.N. & St. John Glew, K.(2019). Isotopic tracking of marine animal movement. In *Tracking Animal Migration with Stable Isotopes* (eds Hobson, K.A., & Wassenaar, L.I.). Academic Press, Cambridge.

Trueman, C.N., MacKenzie, K.M. & Palmer, M.R. (2012). Identifying migrations in marine fishes through stable-isotope analysis. *J. Fish Biol.*, 81, 826–847.

Tsuda, A., Saito, H. & Kasai, H. (2001). Geographical variation of body size of *Neocalanus cristatus*, *N. plumchrus* and *N. flemingeri* in the

subarctic Pacific and its marginal seas: implications for the origin of large form of *N. flemingeri* in the Oyashio area. *J. Oceanogr.*, 57, 341–352.

Urawa, S., Kawana, M., Anma, G., Kamei, Y., Shoji, T., Fukuwaka, M.A. *et al.* (2000). Geographic origin of high-seas chum salmon determined by genetic and thermal otolith markers. *N. Pac. Anadr. Fish Comm. Bull.*, 2, 283–290.

Urawa, S., Azumaya, T., Crane, P.A. & Seeb, L.W. (2005). Origin and distribution of chum salmon in the Bering Sea during the early fall of 2002: estimates by allozyme analysis. *N. Pac. Anadr. Fish Comm. Tech. Rep.*, 6, 67–70.

Urawa, S., Sato, S., Crane, P.A., Agler, B., Josephson, R. & Azumaya, T. (2009). Stock-specific ocean distribution and migration of chum salmon in the Bering Sea and North Pacific Ocean. *N. Pac. Anadr. Fish Comm. Tech. Rep.*, 5, 131–146.

Urawa, S., Ueno, Y., Ishida, Y., Seeb, L.W., Crane, P.A., Abe, S. *et al.* (2001). A migration model of Japanese chum salmon during early ocean life. *N. Pac. Anadr. Fish. Comm. Tech. Rep.*, 2, 45–46.

Wessel, P. & Smith, W.H.F. (1996). A global, self-consistent, hierarchical, high-resolution shoreline database. *J. Geophys. Res.*, 101, 8741–8743.

Whittle, J., Kondzela, C.M., Nguyen, H.T., Hauch, K., Cuadra, D. & Guyon, J.R. (2018). Genetic stock composition analysis of chum salmon from the prohibited species catch of the 2016 Bering Sea walleye pollock trawl fishery and Gulf of Alaska groundfish fisheries. United States Department of Commerce, NOAA Technical. Memorandum, NMFS-AFSC-366.

Yoshikawa, C., Nakatsuka, T. & Wakatsuchi, M. (2006). Distribution of N* in the Sea of Okhotsk and its use as a biogeochemical tracer of the Okhotsk Sea Intermediate Water formation process. *J. Mar. Syst.*, 63, 49–62.

Yoshikawa, C., Makabe, A., Matsui, Y., Nunoura, T. & Ohkouchi, N. (2018). Nitrate isotope distribution in the subarctic and subtropical North Pacific. *Geochem. Geophys. Geosyst.*, 19, 2212–2224.

SUPPORTING INFORMATION

Additional supporting information may be found online in the Supporting Information section at the end of the article.

Editor, Elizabeth Jeffers
Manuscript received 18 November 2019
First decision made 10 January 2020
Manuscript accepted 25 February 2020